Magnetic linear and circular dichroism in core-level photoemission and magnetic circular x-ray dichroism in absorption for ultrathin films Fe/Pd(100)

X. Le Cann, C. Boeglin, and B. Carrière
Institut de Physique et Chimie des Matériaux de Strasbourg Groupe Surfaces-Interfaces, 23 rue du Loess, Boîte Postale 20CR, F-67037 Strasbourg, France

K. Hricovini
Laboratoire pour l'Utilisation du Rayonnement Electromagnétique, Université de Paris-Sud, F-91405 Orsay, France and Université de Cergy-Pontoise, 95011 Cergy-Pontoise, France

(Received 2 October 1995)

Magnetic circular x-ray dichroism (MCXD) experiments have been performed at the Fe $L_{2,3}$ absorption edges on ultrathin bct Fe layer epitaxially grown at room temperature on fcc Pd(100). In the magnetic circular and linear dichroism the asymmetry dependence in the Fe $2p$ and Fe $3p$ photoemission with the thickness of the Fe/Pd(100) film is compared to the simultaneously achieved absorption spectra in the MCXD. The magnetic circular x-ray dichroism results evidence a strong in-plane anisotropy along the [010] direction of the iron film, even for the ultrathin bct iron films grown at room temperature. In the thickness range of 2–3 equivalent monolayers, the magnetic orbital moment of iron is enhanced by a factor 5 [$\langle L_z\rangle=(0.53\pm0.02)\mu_B$] compared to the bulk iron value, whereas the spin moment is meanly unaffected by the interface [$2\langle S_z\rangle=(2.17\pm0.15)\mu_B$]. In core-level photoemission, both linear (Fe $3p$) and circular (Fe $2p$) magnetic dichroism show surprisingly very low asymmetries for 2-ML Fe/Pd(100). This seems to be in contradiction with the analysis of the magnetic dichroic signal at the $L_{2,3}$ Fe edges which leads for this film to a total magnetic moment about $2.70\mu_B$. These measurements offer parameters related to the analysis of magnetic materials with magnetic circular and magnetic linear dichroism techniques. [S0163-1829(96)05525-7]

INTRODUCTION

Magnetic dichroism has become an intensively used technique in the absorption mode as well as in the more surface-sensitive core-level photoemission mode. The first technique opens the interesting possibility to obtain independently the orbital and spin magnetic moment, but is limited by the fact that the information is averaged over a large thickness. Core-level photoemission experiments in magnetic circular and linear dichroism (MCD and MLD) up to now provided a more qualitative magnetic description, and probed the exchange and the spin-orbit coupling. However it suffers from an incomplete understanding, where, for example, the angular dependence of the asymmetry in magnetic circular (and linear) dichroism in the angular distribution MCDAD (and MLDAD) is still in progress.[1–6] On the other hand, besides spin-resolved core-level photoemission, which suffers from low count rates, MCD and MLD in the photoemission mode offer powerful tools to differentiate surfaces, interfaces, and volume contributions in magnetic thin-film systems.

Many interesting results about low-dimensional magnetic systems at surfaces or interfaces have been introduced in the last few years. For thin films or multilayered systems the property of magnetic anisotropy is of the greatest importance. It is essentially governed by the orbital and the spin magnetic moment. In the case of transition metals an increased number of systems have recently been studied where the magnetism at the interfaces or at the surfaces were of interest. In multilayer systems such as Co/Pt, Co/Pd, and Fe/Pd,[7–10] an enhanced magnetic moment at the interface was observed. For the thin films Fe/Cu(100), Co/Cu(100), Mn/Co(100), and Ni/Fe(100),[11–13] an increased orbital magnetic moment has been observed, whereas for the Ni(110) surface a large orbital magnetic moment could be deduced.[14] For the Co/Cu(100) ultrathin film system the surface orbital magnetic moment may be compared to the one obtained in bulk fcc cobalt.[15]

In our paper we will analyze Fe/Pd(100) ultrathin films where each film stays for a complete system with its interface and surface and the related structure (bct and bcc iron). The influence of Fe/Pd interfaces on the magnetic moment of iron was shown by calculations performed for Fe/Pd superlattices by Stoeffler *et al.*,[16] where the moment for each separate layer could be obtained. In this calculation the local spin magnetic moment at the Fe/Pd interface was found to be enhanced to $2.8\mu_B$. This effect is directly related to the $3d$-$4d$ hybridization which affects the majority- and minority-spin bands differently. The enhanced density of spin in the majority-spin band is compensated for by a shifted minority-spin band toward higher energies above the Fermi level, and therefore increases the Fe and the Pd interface local moment. The relative distribution of the Fe and Pd majority- and minority-spin states is at the origin of the magnetic coupling at the interfaces. For systems such as Fe/Pd or Fe/Pt behind the induced moment on the Pd or Pt interface atoms, interesting magnetic property of the ferromagnetic films is the large local magnetic moment at the interfaces ($2.8\mu_B$–$3.1\mu_B$) (Refs. 17–21) compared to alloys.[22] Nevertheless the experiences could mostly not provide quantitative data, or in some cases they were performed on capped bilayers and trilayers with thick Fe films (5–10 ML), where a mixed interface and bulk magnetic signal was observed.[17]

Our aim is to overcome this ambiguity by quantitative magnetic circular x-ray dichroism (MCXD) measurements on ultrathin Fe/Pd(100) layers grown and analyzed *in situ*.

On the other hand, as calculated by Eriksson *et al.*,[23] the bcc iron surface should present an enlarged orbital magnetic moment. Their theoretical values gives for the bcc Fe(100) surface layer an orbital moment of $0.12\mu_B$ instead of $0.05\mu_B$ in the bulk, and an enhanced spin moment $2.87\mu_B$ instead of $2.18\mu_B$ in bulk bcc iron.

For our purpose, an interesting application in the field of thin films is the Fe/Pd(100) thin-film system, for which ferromagnetic order still appears at room temperature for ultrathin films between 1 and 2 ML.[20,24,25] The bct structure of the iron film sets in at the early stage of growth (2 ML).[25,26] In our experiment this means that a total ferromagnetic system at a coverage of 2-ML Fe can be analyzed by two different technics MCD and MCXD, and in this case the information comes from the same iron layers.

For this system (ultrathin films and sandwiches) the localized character of the valence electrons is affected by dimensionality effects at the surface by narrowing of the $3d$-band-width but also at the Fe/Pd interface by $3d$-$4d$ band hybridization. With MCD and MLD in photoemission, we are therefore able to look at the effects of the modified electronic structures introduced by this dimensionality effects.

Magnetic x-ray circular dichroism in the $L_{2,3}$ absorption edge provide a means to accede to an element specific local magnetic moment. Recent theoretical analysis performed in an atomic framework predict that, for $2p$-$3d$ transitions, ground-state expectation values for the spin and orbital moments can be derived.[27,28]

In this paper we will extract the ratio $\langle L_z\rangle/\langle S_z\rangle$ and qualitatively accurate values of $\langle L_z\rangle$ and $\langle S_z\rangle$ by inclusion of the corrections calculated by Wu and Freeman,[31] in order to account differently at the surface or in the ''bulk'' iron film for the neglected $\langle T_z\rangle$ in the application of the sum rules. For the orbital and spin moments we should be almost sensitive to the evolution of these quantities as a function of the film thickness. Furthermore, we show that the MCD signal observed by photoemission is not in direct relation with the Fe $3d$ magnetic moment observed on the Fe $L_{2,3}$ absorption edges. The Fe $2p$ and Fe $3p$ photoemission MCD signal is obviously influenced by the $3d$-$4d$ band hybridization at the Fe/Pd interface. Thus in photoemission the MCD signal is connected to the electronic structure of the occupied d band where $3d$-$4d$ hybridization takes place, and in absorption to the empty d states where hybridization does not much affect the band structure (neglecting sp bands).

EXPERIMENT

MCD experiments were performed at the LURE SuperACO synchrotron facility at the SU23 beam line using the high circular polarization of the light (in our case 70%) produced by an asymmetry hybrid wiggler. The photoemission data were obtained using a constant photon energy of 830 eV for the MCD on the Fe $2p$ line, using σ^+ circularly polarized light, and 200 eV for the MLD on the Fe $3p$ line, using linearly p-polarized light. Both energies were chosen in order to minimize the photoelectron mean free path and to reduce the secondary electron contribution on the row data.

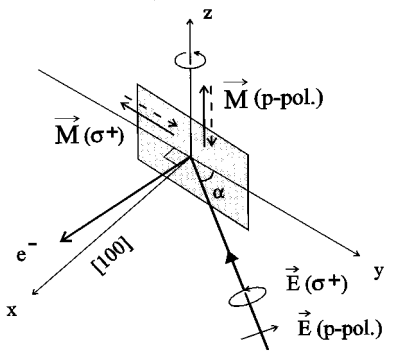

FIG. 1. Geometry of the experiment: MCD and MCXD experiments were achieved using circularly polarized light with a polarization rate of $\tau=70\%$. The incidence angle for the Fe $2p$ MCD experiment was $\alpha=45°$, and the detection of the photoelectron at 5° off normal. The pair spectra were obtained by reversing the in-plane magnetization **M** along the [010] axes of the film which lays in the incidence plane along y. The Fe $3p$ MLD experiments were performed in the same geometry with incoming p-polarized light at $\alpha=45°$ and an in-plane magnetization **M** perpendicular to the incidence plane along the z axis.

Four different monochromator gratings allow a continuous energy scale from low energies ($h\nu=100$–200 eV) to higher photon energies up to 1100 eV. Thus the different spectra could be obtained successively on the same films. The absorption data were collected by measuring the total electron yield and then normalized to a reference photon current.

Fe/Pd(100) has been extensively studied by Liu and Bader[24] by means of *in situ* Kerr rotation. They showed an in-plane easy axis of magnetization along the [100] crystallographic axis of iron films grown at room temperature, with a strong thickness dependence of the Curie temperature T_c which crosses 300 K for near 1-ML Fe/Pd(100). Hysteresis loops in the longitudinal mode shows nearly square loops where for the 3-ML thin films the coercitive field never exceeds 200 Oe. A soft iron yoke was installed *in situ* and it allows an in-plane magnetic field of 300 Oe along the [010] direction of the iron films. A second external system allows perpendicular magnetization and can give fields up to 600 Oe. In our experiment the magnetic saturation of the thin iron films has been obtained by in-plane or out-of-plane current pulses.

The iron films are analyzed in remanence by photoemission on Fe $2p$, Fe $3p$, and Fe $L_{2,3}$ absorption edges. The relative orientation between the light propagation vector and the magnetization direction was reversed by reversing the current in the magnet wires. The geometry of the experiment is shown in Fig. 1. The angle between the sample plane and the light propagation vector was $\alpha=45$. In photoemission the data were recorded with a high-resolution hemispherical energy analyzer for which the acceptance angle was in our experiment of 1.2 in order to accede to angle-resolved data. The photoelectrons were collected at -5 off normal emission along the [100] direction of the iron thin films. This corresponds to a near maximum in the magnetic circular and linear dichroism in the angular distribution (MCDAD and MLDAD).[1–4] The absorption experiments were performed in the same geometry as those of the MCDAD. Different angles

of incidence of the light ($90 \geqslant \alpha \geqslant 30$) were used in order to monitor the saturation effect on the Fe $L_{2,3}$ absorption edges which becomes significant above 10-ML Fe/Pd(100).

Sample preparation and growth of bct Fe/Pd(100)

The Pd(100) sample was cleaned by argon sputtering at 1 kV and 10 μA at 350 °C followed by annealing at 750 °C. This was repeated until the surface show a sharp (1×1) low-energy electron-diffraction (LEED) pattern with a low background and a carbon oxygen free Auger spectrum. The samples were prepared in molecular-beam-epitaxy (MBE) apparatus under UHV conditions ($P<1.10^{-10}$) equipped with LEED and Auger. A quartz microbalance control ensures a constant growth rate of 0.2 ML/min.

The epitaxial growth of the tetragonally distorted bcc phase of the ultrathin iron films has been extensively studied in a separate chamber where the Auger transitions of the Pd (MNN) at 330-eV kinetic energy, and the Fe (LMM) at 651-eV kinetic energy were monitored during the growth. The AS-t curve indicates a strong deviation from a perfect layer-by-layer growth mode still before completion of the first monolayer.[25] The tendency to form islands at room temperature is confirmed when the substrate is cooled to 200 K during the growth by a clear modified AS-t curve which goes toward a layer-by-layer evolution. This has also been confirmed by gently annealing thin films grown at room temperature. For 1-ML Fe/Pd(100) this further treatment leads to an expanded film as could be seen on the Fe and Pd Auger intensities. Our results at room temperature are clearly in contradiction with the Auger studies of the Fe/Pd(100) growth performed by Liu and Bader.[33]

By low-energy electron diffraction we observed relaxation of the strained bct iron film toward a well-ordered bcc structure reached in the 40–50-ML range. The sharp (1×1) LEED spots of the initial Pd(100) surface become broadened with an intense background for the deposition of 1–2-ML iron. After 5-ML Fe/Pd(100) the LEED pattern becomes sharper and the best pattern is seen after a 25-ML deposition. This means that at the first stage of growth the strain induced by the strong distorted bct film induces defects in the islands. The in-plane parameter measured on the LEED spots is constant in the 0–5-ML Fe/Pd(100) range. $I(V)$ curves observed on the 00 spot lead to a surprising constant interlayer distance for 1–5-ML films of 1.95 Å. For 25-ML Fe/Pd(100), the interlayer distance is reduced to 1.48 Å, but remains slightly higher than the bulk bcc Fe value of 1.43 Å.

The structure of Fe/Pd(100) films has previously been studied by means of the $I(V)$ curves by Quinn *et al.*[26] in the range 10–100 ML. They showed that for a 12-ML Fe/Pd(100) film the misfit between the bcc Fe and the 45° rotated fcc Pd(100) leads to a 5% expanded interlayer distances related to the 4.2% in-plane contraction of the bct Fe film, in agreement with our results for 10 ML.

MAGNETIC CIRCULAR DICHROISM IN THE Fe $L_{2,3}$ ABSORPTION EDGES

Magnetic x-ray circular dichroism in the $L_{2,3}$ absorption edges gives a means to accede to an element-specified local magnetic moment. The ground-states expectation values for the spin and orbital moments can be derived from the well-known sum rules[27,28] in the atomic framework. For solids, experimental difficulties related to saturation effects[12,29] or diffuse magnetic moments[30] related to sp moments were examined, and in the case of iron reveal only very small influence on the sum rules extracted values. But even if this holds for the early $3d$ transition metals by neglecting the sp-d wave mixing, we get in trouble in the case of surfaces or interfaces if we neglect the magnetic dipole term.[30–32] The latter is not directly provided by the MCXD experiment for the transition metals. In a noncubic environment the spin magnetic moment, i.e., $2\langle S_z\rangle$, can no longer be approximated by a combination of integrated intensities over the absorption edges. The value of the spin magnetic dipole operator $\langle T_z\rangle$ has to be reconsidered for the surfaces or interfaces where the symmetry is broken. For the considered transitions $(2p\rightarrow3d)$, where the angular momentum of the initial core state is 1 and of the final valence state is 2, the spin sum rule is given by the relation

$$\frac{\int_{L_3}[\sigma_+(\hbar\omega)-\sigma_-(\hbar\omega)]d\hbar\omega-2\int_{L_2}[\sigma_+(\hbar\omega)-\sigma_-(\hbar\omega)]d\hbar\omega}{\int_{L_3+L_2}[\sigma_+(\hbar\omega)+\sigma_-(\hbar\omega)+\sigma_0(\hbar\omega)]d\hbar\omega}=\frac{\langle S_z\rangle+7\langle T_z\rangle}{3n_h}, \tag{1}$$

where n_h denotes the number of valence holes, and σ_+ and σ_- the absorption cross section for the incident light polarized respectively parallel and antiparallel along the direction of magnetization. σ_0 denotes the isotropic absorption cross section, which is taken as $(\sigma_+ + \sigma_-)/2$. Figure 2 shows the Fe $L_{2,3}$ absorption spectra of a 2-ML Fe/Pd(100) film normalized to 100% circular polarization of the light. We plot also the difference spectrum for the grazing ($\alpha=35°$), and for the normal incidence of the light. These data show that for these experimental conditions no perpendicular magnetic domains exists at low coverages. This result is important for two reasons: (i) The magnetic spin and orbital contributions deduced by the application of the sum rules depends on the relative orientation of the moment to the incident light propagation vector. (ii) In photoemission, MCDAD and MLDAD are both very sensitive to the orientation of the magnetic moment in respect with the incoming photon and the emitted photoelectron.[1–6,14]

The observed dichroic signal at room temperature is zero for 1-ML Fe/Pd(100) related to the lower $T_{c(1\,\mathrm{ML})}$ for this film thickness. The onset for the magnetic signal lays between 1 and 1.5 ML, as seen in Fig. 3 (right axis), where the normalized Fe MCXD intensity at the L_3 edge is shown as a function of the film thickness. The normalized MCXD is

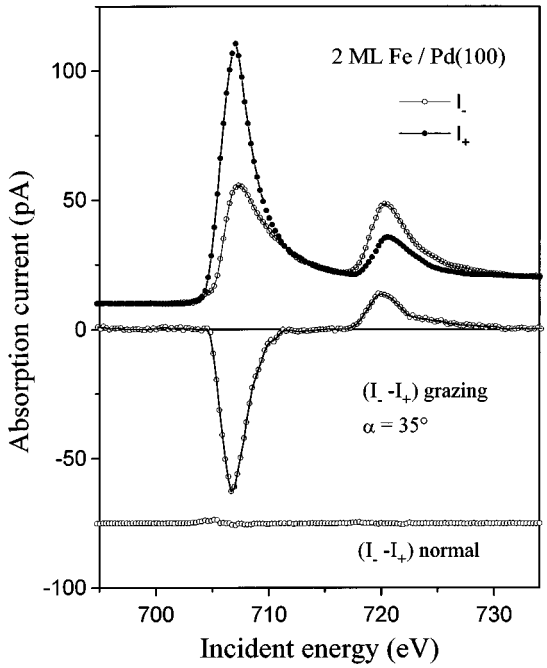

FIG. 2. Fe $L_{2,3}$ x-ray absorption edges for the two opposite in-plane magnetization directions normalized to 100% circularly polarized light, and the difference spectra obtained for grazing ($\alpha = 35°$) and normal incidence ($\alpha = 90°$) of the light for 2-ML Fe/Pd(100).

defined as in Ref. 15 and represents the MCXD difference spectrum over the linear absorption intensity at the L_3 edge. The evolution of the normalized Fe MCXD intensity at the Fe L_3 edge is used to monitor the degree of the long-range magnetic order in the remanent film. The drawn line shows a

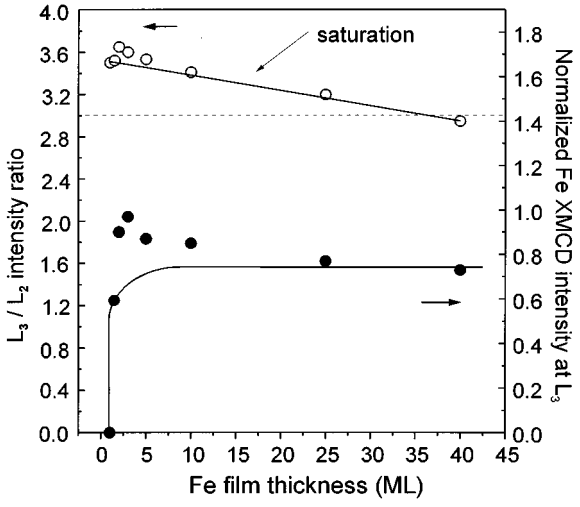

FIG. 3. Left axis: Magnitude of the linear x-ray-absorption intensity ratio $I(L_3)/I(L_2)$ as a function of film thickness compared to the saturation effect introduced by the depth dependence to the cross section $\sigma(L_3)$ and $\sigma(L_2)$ assuming a homogeneous iron film and an effective escape depth of the secondary electrons $\lambda_e(L_{2,3}) = 17$ Å. Right axis: The magnetic dichroism signal $(\sigma^- - \sigma^+)$ at the Fe L_3 edge normalized to the total absorption intensity at the L_3 edge as a function of the Fe thickness.

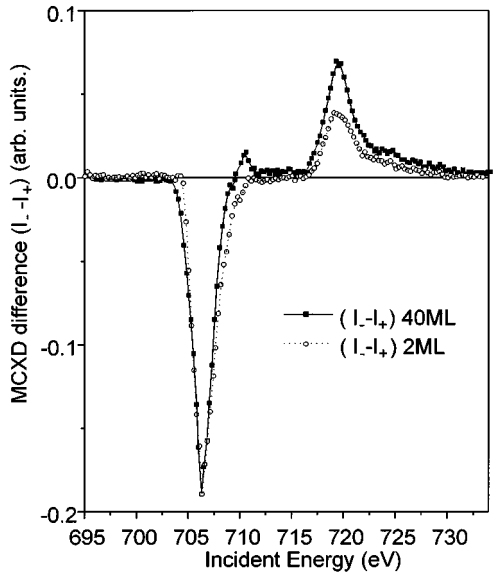

FIG. 4. The MCXD signal $(\sigma^- - \sigma^+)$ and the fine structure between the L_3 and L_2 edges for an ultrathin film Fe/Pd(100) compared to the 40-ML film. The two difference spectra are normalized at the Fe L_3 edge.

typical evolution of the normalized MCXD intensity, as can be observed for the Co/Cu(001) thin films.[12] The normalized difference spectrum observed for 1.5 ML is obviously reduced compared to the thicker film signal. This is related to an imperfectly magnetized film at room temperature. This is in agreement with earlier calibration from Rader *et al.*,[20] where the first nonvanishing spin polarization at the valence band has been found at 1.3-ML Fe/Pd(100). The enhanced values for the 2–10-ML films are either an indication of an enhanced magnetic ordering in these remanent films or of an enhanced local magnetic moment in the low-dimensional films. In fact the latter is confirmed if we consider the evolution of the magnitude of the linear x-ray-absorption intensity ratio $R = L_3/L_2$ in this specific thickness range (Fig. 3, left axis). We compare these data to an estimated evolution of R between 1- and 40-ML Fe/Pd(100), considering saturation effects with an effective escape depth of $\lambda = 17$ Å. Thus we notice a parallel evolution of the linear absorption ratio up to 40 ML, and the saturation effect. But for the film at 2–5-ML coverage this linearity seems to fail. Thus the evolution of the relative L_3/L_2 difference intensity starting from the 2-ML sample and compared with the 40-ML film is an indication of an enhanced orbital moment for our ultrathin Fe films.

For further investigation we apply the sum rules[27,28] and perform the integration over the difference spectra. In Fig. 4 we show two representative difference spectra. Note the absence of positive structure between 710 and 715 eV for the ultrathin 2-ML film compared to the structure observed for our ''bulklike'' 40-ML Fe/Pd(100), or the very similar spectrum given by Chen.[34] This is confirmed for all our thin films up to almost 25 ML. Simultaneously the linear x-ray-absorption spectra shows a smooth out of the ''fine structure'' on the high-energy side of the L_3 edge (see Fig. 6) for the ultrathin films (2–10 ML). The similarity of the observed structures can be tentatively assigned to diffuse MCXD seen

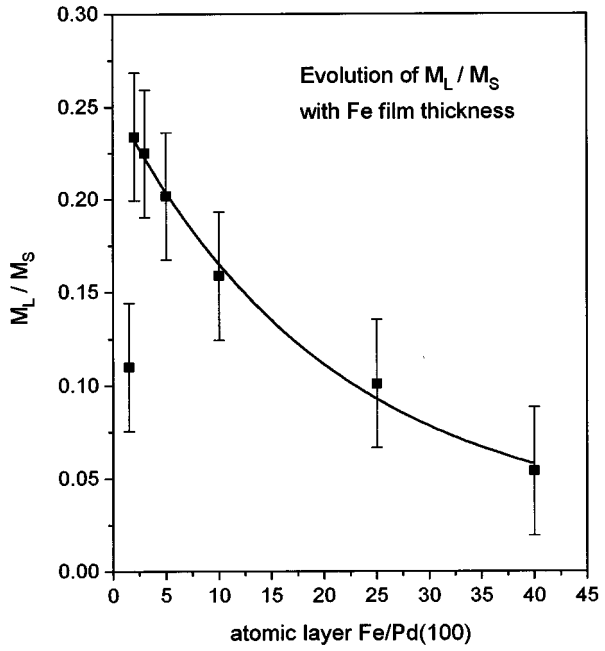

FIG. 5. The orbital to spin moment ratio $Ro/s=M_L/M_S$ as a function of the iron coverage at room temperature.

in the case of Co $L_{2,3}$ and Ni $L_{2,3}$ edges.[30] The absence of positive fine structure in the difference spectra between the L_2 and L_3 edges of our thin films could therefore be related to the importance of oppositely polarized empty ''*s*'' final states relative to the empty 3*d* final states. The extent of the *s*-*p* band obviously contributes to the difference observed for the 2-ML film over a wide range of energy including the L_3 and L_2 edges. Nevertheless the spectra demonstrate that the area under the L_2 peak is smaller for the 2-ML film compared to the one observed for 40 ML by scaling the two spectra at the L_3 edges. Qualitatively this reveals a difference in the magnetism between the 2- and 40-ML thin films.

Integration over the difference spectra gives rise, without any parameter input in our case, to the $\langle L_z\rangle/\langle S_z\rangle$ ratio, assuming that for all our thin iron films the magnetic dipole operator $\langle T_z\rangle$ can be neglected. In fact the perturbation introduced for the $\langle L_z\rangle/\langle S_z\rangle$ ratio is the factor $(1-7\langle T_z\rangle/2\langle S_z\rangle)$ which is given by the first sum rule. For bcc iron, first-principles band-structure calculations[31] provide a ratio $\langle T_z\rangle/\langle S_z\rangle$ of 0.003 which introduces a correction factor of 0.99. This justifies that for the $\langle L_z\rangle/\langle S_z\rangle$ ratio we neglect $\langle T_z\rangle$. At the surfaces and interfaces of the ultrathin Fe/Pd(100) films, this is still correct because the correction calculated by Wu *et al.*[31] is of the same order of magnitude in the case of the bcc Fe(100) surface.

The orbital to spin ratio $\langle L_z\rangle/2\langle S_z\rangle$ obtained by application of the first sum rule is shown in Fig. 5, where the evolution toward a near-bulklike ratio of 0.05 is observed for the 40-ML iron film. The ultrathin iron films show strong enhancement of the $\langle L_z\rangle/2\langle S_z\rangle$ ratio which reaches a maximum value of 0.24 at 2-ML Fe/Pd(100), corresponding to a five times higher value as for bulk bcc iron given at 0.043 by Chen *et al.*[34] This results from the enhanced orbital moment due to the hybridization at the Pd interface.

The individual evolution of orbital and spin moments

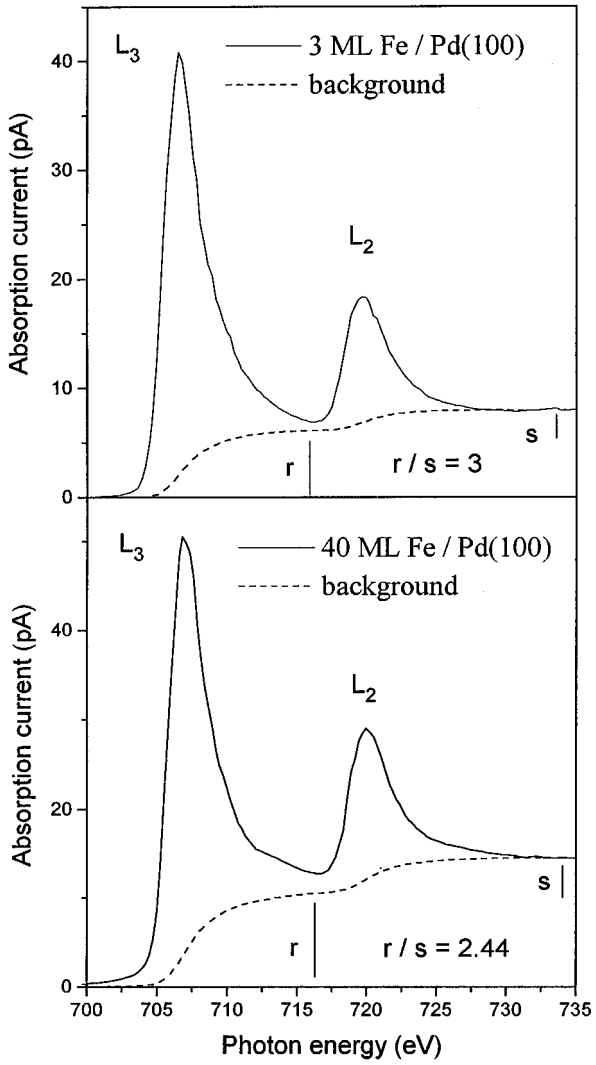

FIG. 6. Fe $L_{2,3}$ total absorption edges for 3-ML Fe/Pd(100) and for 40-ML Fe/Pd(100) with their respective adjusted background. The jump of the step between L_3 and L_2 is defined by the integrated L_3 over the integrated L_2 value which is related through the saturation effect to the iron film thickness.

needs further treatment of the data. The background of the isotropic spectrum has been calculated self-consistently by a two-steplike function as shown in Fig. 6 for the integration of the summed spectra $(I_+ + I_-)$ over the two edges L_3+L_2. The first ''step'' between L_3 and L_2 edges do not reach the experimental curve at 717 eV but stay at a lower level defined by a ratio r/s (see Fig. 6) depending on the L_3/L_2 ratio ($r/s=2.44$ for 40 ML and $r/s=3.0$ for 3 ML). The set of parameters which accounts for the absolute values of spin and orbital moments are the circularly polarization rate τ of the light, the hole number in the Fe 3*d* band n_h and the incidence angle α as well as the azimuthal angle φ [defined as the angle between the [010] direction in the plane of the Fe film and the incidence plane defined by (x,y) (Fig. 1)]. The hole number in the *d* band n_h (3.49/atom) is taken independent of the thickness of the films. In our experiments we used $\alpha=45°$ and 35°, $\varphi=0°$, and $\tau=70\%$. The extracted values of $\langle L_z\rangle$ and $\langle S_z\rangle$ by setting $\langle T_z\rangle=0$ were cor-

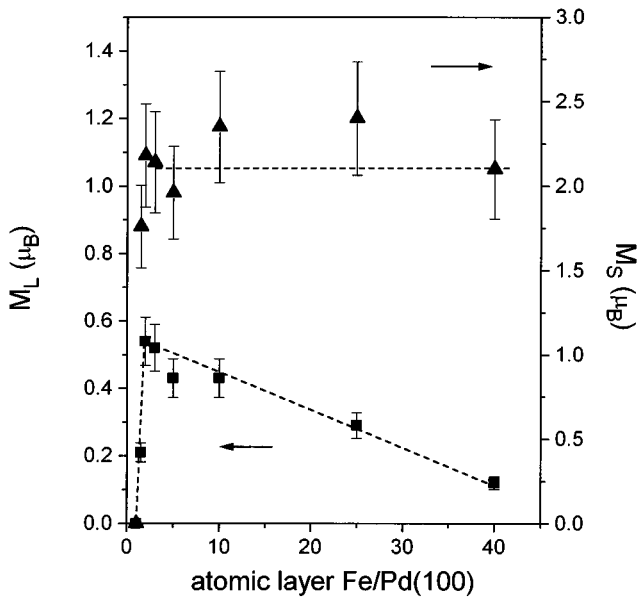

FIG. 7. Evolution of the spin magnetic moment (right scale) and of the orbital magnetic moment (left scale) with the film thickness at room temperature. The values are obtained by application of the sum rules on the Fe $L_{2,3}$ edges with the calculated corrections accounting for the magnetic dipole operator $\langle T_z \rangle$ at the surface, interfaces, and in the bulk of the thin iron films.

rected by the calculated deviation accounting for $\langle T_z \rangle$, at the surface and in the bulk of the iron film as given by Wu *et al.*[31]

The evolution of the orbital and of the spin moment given in Fig. 7 clearly shows a continue decrease of the orbital contribution from $0.54\mu_B$ for 2 ML toward $0.12\mu_B$ for 40 ML and an almost constant spin moment. If we consider that the ''transfer of orbital moment'' from Pd into the iron film concerns more than the first Fe layer at the interface, we obtain a long-range evolution as seen on the ratio Ro/s and on $\langle L_z \rangle$. Thus the strongly enhanced orbital moment is related to the underlying Pd(100). The error bars on the spin value are very large, and thus we are not able to give a conclusive indication as to a thickness-dependent spin moment.

Application of the sum rules leads to a total magnetic moment of $2.72\mu_B$ for 2-ML Fe/Pd and $2.67\mu_B$ for 3-ML Fe/Pd(100). This strong enhanced total magnetic moment in the bct Fe films is in agreement with recent polarized neutron reflection and ferromagnetic resonance experiments,[9] which give layer-averaged total moment values of $2.66\mu_B$ for gold-capped Pd/5.6 ML Fe/Ag(001) samples. The observed enhancement of the total magnetic moment M_L+M_S at low coverages is thus related to the enhanced orbital moment at the near interface region. The in-plane anisotropy observed for all films grown and analyzed at room temperature has been attributed in a previous work[25] to strong reduction of the magnetocrystalline surface anisotropy induced by the morphology of the film.

MCD IN PHOTOEMISSION

In order to separate qualitatively the contribution of the surface and of the Fe/Pd interface, we archived magnetic

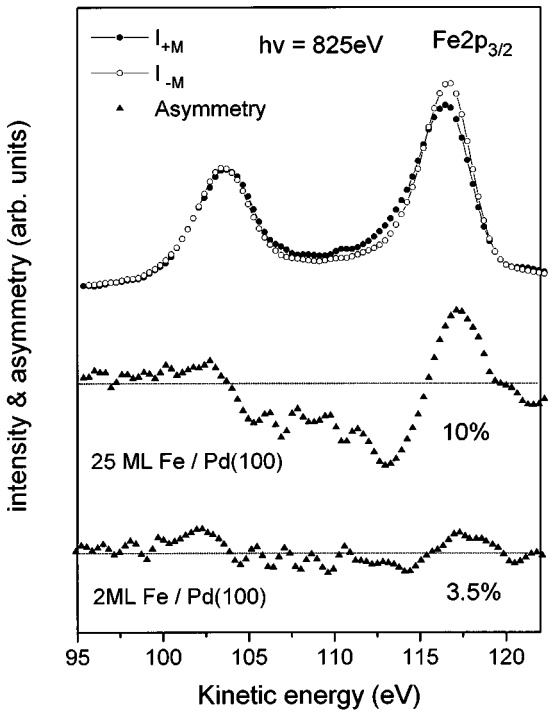

FIG. 8. Fe $2p$ photoemission spectra taken at 825-eV photon energy for circularly polarized light σ^+ obtained for the two directions of the sample magnetization [parallel (●) and antiparallel (○) to the polarization vector of the light] and for 25-ML Fe/Pd(100) at room temperature. The asymmetry $(I_- - I_+)/(I_- + I_+)$ obtained for the 25-ML film is 10%. At the lower part of the figure we show the compared reduced value of the asymmetry (3.5%) obtained for a 2-ML iron film.

circular dichroism (MCD) in photoemission on the Fe $2p$ core levels, where the mean free path is of the order of 5 Å. In this experiment the photon energy was chosen at $h\nu = 825$ eV in order to keep the kinetic energy of the detected photoelectrons at a low value (110 eV), out of the secondary electrons region. In MCD the magnetic signal is currently given by the asymmetry defined by the ratio $A=(I^+ - I^-)/(I^+ + I^-)$. In order to compare our data with earlier work,[2,3] we subtract a Shirley background from the two photoemission spectra $I^+(E)$ and $I^-(E)$, and normalize all of them to a signal-to-background ratio of 2, as seen in Fig. 8 for the pair spectrum obtained for 25-ML Fe/Pd(100). The data were recorded in the geometry where the light incidence angle was 45° with respect to the surface ($\alpha = 45°$), and the photoelectron emission angle at $-5°$ from the normal of the sample as shown in Fig. 1. Circularly polarized light of positive helicity (σ^+) with a 70% polarization rate was used. Thus the normalized asymmetries shown in Fig. 8 are directly comparable to those obtained in earlier works[2,3] obtained in this geometry. As seen in Fig. 8, a surprisingly low asymmetry of 3.5% is observed for 2-ML Fe/Pd(100) compared to the 10% in the 25-ML film. Intermediate thicknesses of iron shows intermediate asymmetries [10-ML Fe/Pd(100), for example, shows $A=7\%$]. The value for the 2-ML film is noticeably lower than the previously measured 10% asymmetry, on the Fe(100) single crystal[2] or on the polycrystalline iron film.[3] Thus for the ultrathin 2-ML film a reduced asymmetry by a factor 3 is observed com-

pared to the thicker 25-ML film and the Fe(100) single crystal. This anomalously low asymmetry of 3.5% is independent of incomplete remanence because the data were obtained on the same 2-ML film and with the same magnetization process as for the Fe $L_{2,3}$ absorption measurements. Contamination of the ultrathin iron film can be excluded by a final MCXD absorption control on the Fe $L_{2,3}$ edges at the end of the typically 3-h acquisition for the photoemission experiment achieved under ultrahigh vacuum conditions. The theoretical value of the magnetic moment averaged over the three outermost surface planes in Fe(100) single crystal is $2.6\mu_B$, and provides a 10% asymmetry in our geometry. The 2-ML iron film by MCXD shows a overaged magnetic moment of $2.7\mu_B$, but stays far from the expected MCD asymmetry. Even if this film shows small islands[25] the sensitivity ($\lambda = 5$ Å) of the photoemission allows an analysis of the whole iron film at this coverage. The tetragonal distorted bct structure is also of minor importance in respect of angular sensitivity of the MCDAD (10% distortion of the out-of-plane and 5% for the in-plane parameter implies a 6° rotation of the atomic row [110] in respect of the light incidence). Thus the influence of the Fe/Pd interface seems to be the most important perturbation we introduce in the MCD detection.

In order to separate the Fe/Pd interface contribution form the ultrathin film surface effect, we achieved Pd/Fe/Pd(100) sandwiches in the MLDAD on the Fe $3p$ core levels in order to reach a better sensitivity in the variation of the asymmetry. The thickness evolution of the asymmetry observed with circularly polarized light has been confirmed on Fe $3p$ with linearly polarized light (Fig. 9) in the geometry where the magnetization vector M lies along the z axes (see Fig. 1). We obtain the bulk expectation value at $h\upsilon = 200$ eV (Ref. 35) of 17% asymmetry for 40-ML Fe/Pd(100) (compatible to the absorption experiments) but the Fe $3p$ asymmetry for the 3-ML Fe/Pd(100) film seems to be again reduced by a factor 5 compared to the thickest film. If we compare the Fe $3p$ MLDAD signal of the uncovered 40-ML Fe/Pd(100) film with the 1-ML Pd/40-ML Fe/Pd(100) sandwich, where the iron located at the top Pd/Fe interface makes the major contribution in the MLDAD, then we are sensitive to the isolated Pd/Fe interface. The 1-ML Pd film covers by a flat epitaxial film the underlying iron. The perfect layer-by-layer growth of Pd/Fe(100) has been observed by mean of Auger and LEED during our experiment, and is confirmed by Celinski.[17] If we compare the Fe $3p$ dichroic signal (Fig. 9) to the one obtained for 40-ML Fe/Pd(100) we again see a strong decrease of the MLDAD asymmetry ($A = 7\%$) as seen for the thinnest Fe/Pd(100) film. This leads to the conclusion that the Fe/Pd interfaces are at the origin of the reduced asymmetries seen by photoemission (MCDAD and MLDAD). Furthermore, we explain the difference in the asymmetries between 3 ML (3%) and the sandwich (7%) by considering the morphology of the thin iron film. The 3-ML iron film shows islands where the topmost layered atoms are located between the fifth layer down to the first interface layer. In our experiment, where the most important contribution in the Fe $3p$ signal comes from the two topmost iron layers, the photoelectrons comes from these different steps, and thus the MLDAD is a mixture of this arrangement. For the sandwich Pd/40-ML Fe/Pd(100) the sharp interface can

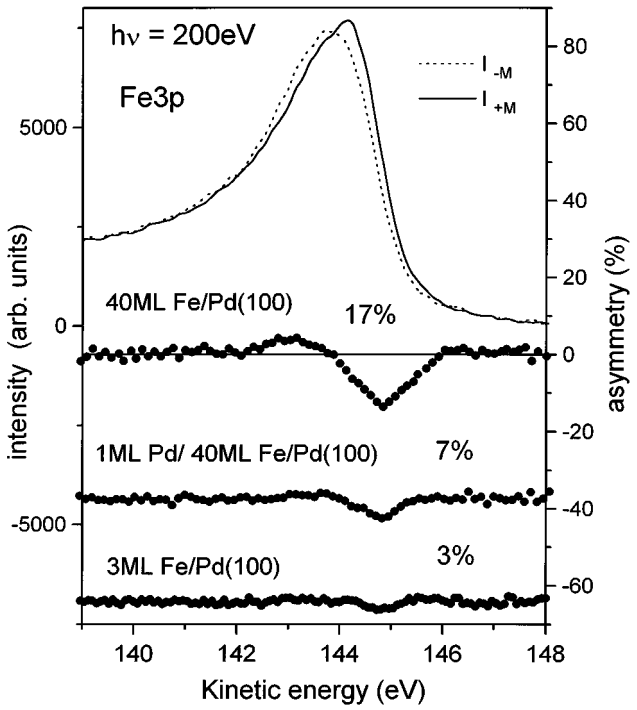

FIG. 9. Fe $3p$ photoemission spectra taken at 200-eV photon energy for linearly polarized light obtained for the two directions of the sample magnetization perpendicularly to the incidence plane for 40-ML Fe/Pd(100). The value of the asymmetry (right scale) obtained by MLD is of 17% for the 40-ML film, whereas a clear reduced asymmetry is observed for the sandwich (7%) and for the ultrathin film of 3 ML.

therefore explain the 7% asymmetry on the Fe $3p$. Nevertheless the meaning of the strongly reduced asymmetry observed by MCDAD and MLDAD at the interfaces and ultrathin films is not yet clear.

Compared to the absorption data obtained at 2 and 3 ML, the MCD and MLD experiments on core levels are obviously not able to provide direct indication on the magnetic moment. In the particular case of the Fe/Pd interface the band hybridization in the occupied $3d$-$4d$ band obviously plays a key role.

The extent of the induced orbital moment from the Pd layers into the iron film seen by MCXD can be speculatively compared to the extent of the reduced asymmetry in MCD and MLD in core-level photoemission. Nevertheless, no direct connection between the two parameters can be thought of in terms of reduced asymmetries for enhanced orbital magnetic moments. Our results in MCD and MLD indeed show a more complex signal than the MCXD in absorption. The photoemission is well known to be sensitive to the exchange energy ζsS between the core level and valence band, and for this reason shows a dependence on both the local spin moment and the exchange constant ζ. This value is band structure dependent and changes upon d-band state mixing. Thus the changes in the asymmetries observed by MCD and MLD in our thin films and sandwiches could be related to the influence of the electronic structure of the Pd/Fe interface on the exchange energy.

CONCLUSION

We have presented magnetic dichroism results at room temperature on Fe/Pd(100). The main conclusion obtained by MCXD in absorption is the strong increase of the orbital magnetic moment for ultrathin Fe/Pd(100) films, which is in agreement with the enhanced total magnetic moment previously observed and with theoretical results at the Fe/Pd interfaces. For the ultrathin films, different conclusions on the magnetic long-range order could be given if we consider the MCXD results from the Fe $L_{2,3}$ absorption data or the core-level photoemission (Fe $2p$ and Fe $3p$) in MCD and MLD experiments. Even if the discrepancy is not understood, these experiments show that the MCD and MLD in core-level photoemission are far from a simple experimental fingerprint of magnetic thin films, surfaces, and interfaces.

[1] D. Venus, L. Baumgarten, C. M. Schneider, C. Boeglin, and J. Kirschner, J. Phys. Condens. Matter **5**, 1239 (1993).
[2] L. Baumgarten, thesis, Freie Universität, Berlin, 1992.
[3] C. Boeglin, E. Beaurepaire, V. Schorsch, B. Carrière, K. Hricovini, and G. Krill, Phys. Rev. B **48**, 13 123 (1993).
[4] D. Venus, Phys. Rev. B **48**, 6144 (1993).
[5] H. B. Rose, F. U. Hillebrecht, E. Kisker, R. Denecke, and L. Ley, J. Magn. Magn. Mater. **148**, 62 (1995).
[6] G. Van der Laan, Phys. Rev. B **51**, 240 (1995).
[7] Y. Wu, J. Stöhr, B. D. Hermsmeier, M. G. Samant, and D. Weller, Phys. Rev. Lett. **69**, 2307 (1992).
[8] D. Weller, Y. Wu, J. Stöhr, M. G. Samant, B. D. Hermsmeier, and C. Chappert, Phys. Rev. B **49**, 12 888 (1994).
[9] J. A. C. Bland, C. Daboo, B. Heinrich, Z. Celinski, and R. D. Bateson, Phys. Rev. B **51**, 251 (1995).
[10] E. E. Fullerton, D. Stoeffler, K. Ounadjela, B. Heinrich, Z. Celinski, and J. A. C. Bland, Phys. Rev. B **51**, 6364 (1995).
[11] J. G. Tobin, G. D. Wadill, and D. P. Pappas, Phys. Rev. Lett. **68**, 3642 (1992).
[12] W. L. O'Brien and M. P. Tonner, Phys. Rev. B **50**, 2963 (1994).
[13] J. Vogel, G. Panaccione, and M. Sacchi, Phys. Rev. B **50**, 7157 (1994).
[14] G. Van deer Laan, M. A. Hoyland, M. Surman, C. F. J. Flipse, and B. T. Thole, Phys. Rev. Lett. **69**, 3827 (1992).
[15] M. Tischer, O. Hjortstam, D. Arvanitis, J. Hunter Dunn, F. May, K. Baberschke, J. Trygg, J. M. Wills, B. Johansson, and O. Eriksson, Phys. Rev. Lett. **75**, 1602 (1995).
[16] D. Stoeffler, K. Ounadjela, J. Sticht, and F. Gautier, Phys. Rev. B **49**, 299 (1994).
[17] Z. Celinski, B. Heinrich, J. F. Cochran, W. B. Muir, A. S. Arratt, and J. Kirschner, Phys. Rev. Lett. **65**, 1156 (1990).
[18] W. Weber, D. A. Wesner, G. Guntherodt, and U. Linke, Phys. Rev. Lett. **66**, 942 (1991).
[19] O. Rader, C. Carbone, W. Clemens, E. Vescovo, S. Blügel, W. Eberhardt, and W. Gudat, Phys. Rev. B **45**, 13 823 (1992).
[20] O. Rader, E. Vescovo, J. Redinger, S. Blügel, C. Carbone, W. Eberhardt, and W. Gudat, Phys. Rev. Lett. **72**, 2247 (1994).
[21] M. Finazzi, L. Braicovich, C. Roth, F. U. Hillebrecht, H. B. Rose, and E. Kisker, Phys. Rev. B **50**, 14 671 (1994).
[22] J. F. van Acker, P. J. W. Weijs, J. C. Fuggle, K. Horn, H. Haak, and K. H. J. Buschow, Phys. Rev. B **43**, 8903 (1991), and references therein.
[23] O. Eriksson, A. M. Boring, R. C. Albers, G. W. Fernando, and B. R. Cooper, Phys. Rev. B **45**, 2868 (1992).
[24] C. Liu and S. D. Bader, Phys. Rev. B **44**, 2205 (1991).
[25] X. Le Cann, C. Boeglin, K. Hricovini, and B. Carrière (unpublished).
[26] J. Quinn, Y. S. Li, H. Li, D. Tian, F. Jona, and P. M. Marcus, Phys. Rev. B **44**, 3959 (1991).
[27] B. T. Thole, P. Carra, F. Sette, and G. van der Laan, Phys. Rev. Lett. **68**, 1943 (1992).
[28] P. Carra, T. Thole, M. Altarelli, and X. Wang, Phys. Rev. Lett. **70**, 694 (1993).
[29] J. Vogel and M. Sacchi, Phys. Rev. B **49**, 3230 (1994).
[30] W. L. O'Brien and B. P. Tonner, Phys. Rev. B **50**, 12 672 (1994).
[31] R. Wu, D. Wang, and A. J. Freeman, Phys. Rev. Lett. **71**, 3581 (1993); R. Wu and A. J. Freeman, *ibid.* **73**, 1994 (1994).
[32] R. Wu, D. Wang, and A. J. Freeman, J. Magn. Magn. Mater. **132**, 103 (1994).
[33] C. Liu and S. D. Bader, J. Magn. Magn. Mater. **93**, 307 (1991).
[34] C. T. Chen, Y. U. Idzerda, H. J. Lin, N. V. Smith, G. Meigs, E. Chaban, G. H. Ho, E. Pellegrin, and F. Sette, Phys. Rev. Lett. **75**, 152 (1995).
[35] G. Rossi, F. Sirotti, N. A. Cherepkov, F. Combert Farnous, and G. Panaccione, Solid State Commun. **90**, 557 (1994).